Defect formation in the Swift-Hohenberg equation

Tobias Galla[1,*] and Esteban Moro[1,2,†]

[1]*Theoretical Physics, University of Oxford, 1 Keble Road, Oxford OX1 3NP, United Kingdom*

[2]*Departamento de Matemáticas and GISC, Universidad Carlos III de Madrid, Avenida Universidad 30, 28911 Leganés, Spain*

(Received 26 November 2002; published 12 March 2003)

We study numerically and analytically the dynamics of defect formation during a finite-time quench of the two-dimensional Swift-Hohenberg (SH) model of Rayleigh-Bénard convection. We find that the Kibble-Zurek picture of defect formation can be applied to describe the density of defects produced during the quench. Our study reveals the relevance of two factors: the effect of local variations of the striped patterns within defect-free domains and the presence of both pointlike and extended defects. Taking into account these two aspects we are able to identify the characteristic length scale selected during the quench and to relate it to the density of defects. We discuss possible consequences of our study for the analysis of the coarsening process of the SH model.

The formation of topological defects in symmetry-breaking phase transitions is a very generic phenomenon in physics, and can be studied analytically and experimentally in different condensed matter systems [1,2]. An example is the onset and formation of stripe patterns in the Rayleigh-Bénard convection [2,3]. In this paper, we focus on the Swift-Hohenberg (SH) model [4] for this process. Once above the convective threshold, the system develops a labyrinthine morphology, consisting of domains of stripes that are oriented along arbitrary directions [5]. Between those domains, the system displays several types of topological defects, such as grain boundaries, disclinations, and dislocations. This structure orders with time basically by grain boundary relaxation and defect annihilation. Similar to other models, in which this coarsening process is self-similar [6], any linear scale of the structure is expected to grow as a power law in time $\xi \sim t^{1/z}$. However, simulations of sudden quenches of the SH equation [7–12] have revealed that the observed exponent z is sensitive to nonuniversal model features such as the quench depth or noise strength. Moreover, different definitions of the length scale have led to different exponents with values reported in the interval $2 \leq z \leq 5$. This apparent absence of self-similarity in the coarsening is also found in related experiments of electroconvection [13] and diblock copolymers [14]. Multiscaling [10,13] and/or defect pinning [11] have been proposed as being responsible for the scattered value of z, but no general picture has been reached so far about the true nature of the coarsening process.

In this paper we consider a complementary, but related aspect of the nonequilibrium dynamics of the SH equation. Namely, we are interested in the formation of defects in a finite-time quench (annealing). Interestingly, some features of finite-time quenches were considered in some early works comparing the SH model with the Rayleigh-Bénard experiments [15]. Specifically, we study situations in which the control parameter, the reduced Rayleigh number $\varepsilon \equiv (R - R_c)/R_c$, is swept smoothly over the bifurcation point, ε

$=0$. Our study is thus related to earlier papers on defect formation in nonequilibrium second-order phase transitions [16–18]. The theoretical picture which is believed to be applicable in this case is the Kibble-Zurek mechanism [16]: because of critical slowing down close to the transition point, the system cannot follow the external change of the critical parameter and the dynamics are suspended in an interval $[-\hat{\varepsilon}, \hat{\varepsilon}]$ around the transition. After this suspension a characteristic length ξ is selected and is found to scale with the rate of increase μ of the critical parameter like $\xi \sim \mu^{-\gamma}$. In particular, mean-field theory predicts $\hat{\varepsilon} \sim \mu^{1/2}$ and $\xi \sim \mu^{-1/4}$ for models of the Ginzburg-Landau type with $O(N)$ symmetry [16]. This length ξ sets an initial density of defects, ρ, directly after the quench. Within a Gaussian approximation one expects $\rho \sim \xi^{-2}$ for pointlike defects and $\rho \sim \xi^{-1}$ for line defects in two dimensions [19]. Thus, the Kibble-Zurek mechanism predicts that the density of defects observed directly after the quench scales with μ as well, as confirmed in various models [17,18,20].

The purpose of this paper is to confirm the validity of the Kibble-Zurek scenario for the SH model. To this end, we identify the characteristic length ξ selected during the annealing process and study its relation to the density of defects. We model the annealing protocol of the Rayleigh-Bénard system by the SH equation in two dimensions and in dimensionless variables [2,4]

$$\partial_t \phi = \varepsilon(t)\phi - (q_0^2 + \nabla^2)^2 \phi - \phi^3 + \eta, \qquad (1)$$

where $\varepsilon(t) = \mu t$. This corresponds to an experimental situation where the temperature difference between the upper and the lower plate of the convection cell is increased linearly in time. The order parameter field $\phi(\mathbf{x}, t)$ is related to the vertical fluid velocity. The last term in Eq. (1) is a stochastic forcing term, with $\langle \eta(\mathbf{x}, t)\eta(\mathbf{x}', t')\rangle = 2F\delta(\mathbf{x} - \mathbf{x}')\delta(t - t')$, where the noise strength $F = 5 \times 10^{-17}$ is compatible with typical experimental values [4,15]. Our simulations are performed on a square lattice of 512×512 nodes with lattice spacing $\Delta x = \pi/4$, corresponding to eight lattice points per

*Electronic address: galla@thphys.ox.ac.uk
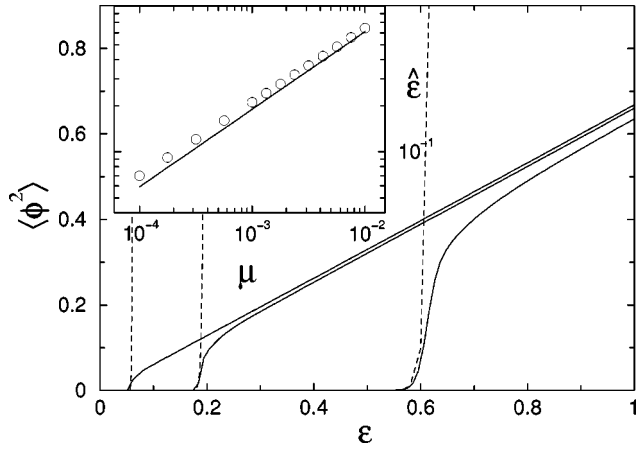
†Electronic address: emoro@math.uc3m.es

FIG. 1. Variance of the order parameter $\langle \phi^2 \rangle$ obtained from the simulations (solid lines) compared with the linear approximation given by Eq. (5) (dashed lines) with $\mu = 10^{-4}$, $\mu = 10^{-3}$, and $\mu = 10^{-2}$ from left to right. Inset, numerical values of $\hat{\varepsilon}$ as a function of μ obtained implicitly from $\langle \phi^2 \rangle = \delta \hat{\varepsilon}$ with $\delta = 1/2$. The solid line is the prediction of Eq. (6).

ideal wavelength ($q_0 = 1$). Initial conditions are $\phi(\mathbf{x}, t_0) = 0$ at the instant t_0 given by $\varepsilon(t_0) = -1/2$.

As the critical parameter ε is increased in time the magnitude of the order parameter remains close to $\phi = 0$ until well after the onset of the instability at $\varepsilon = 0$ (see Fig. 1). At some later instant $\varepsilon = \hat{\varepsilon} > 0$ the field abruptly jumps towards its symmetry-broken quasiequilibrium at $\langle \phi^2 \rangle = 2\varepsilon(t)/3$ and spatially periodic modulations of the signal are created, see Fig. 2. We identify the instant $\hat{\varepsilon}$ at which dynamics are resumed as the time when $\langle \phi^2 \rangle = \delta \hat{\varepsilon}$ [18] [with $\delta = O(1)$, meaning that the first and third term on the right-hand side of Eq. (1) are of equal importance]. Results are presented in Fig. 1 where we find $\hat{\varepsilon} \sim \mu^{0.48 \pm 0.01}$, which compares well with the Kibble-Zurek predicted scaling $\hat{\varepsilon} \sim \mu^{1/2}$. It is interesting to note that the same scaling was found in ramp experiments of the Rayleigh-Bénard convection [15], where the temperature difference between the upper and lower plate of
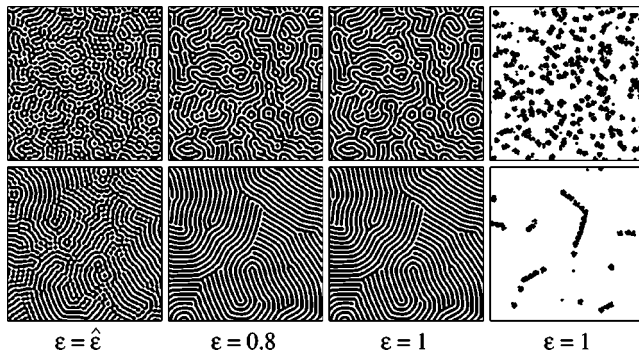

FIG. 2. Typical configurations of the order parameter field for different values of ε. We depict an area of 256×256 lattice points. Upper row, $\mu = 10^{-2}$, lower row $\mu = 10^{-4}$. Black (white) points correspond to $\phi > 0$ ($\phi < 0$). Rightmost panels display the defect structures obtained from the amplitude signal ($\vartheta = 0.25$, see text).
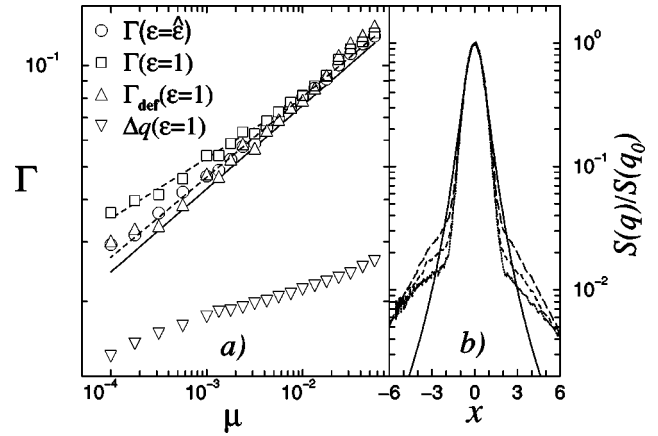

FIG. 3. (a) Width of the structure factor Γ after the quench compared with the local variations of the wave number Δq. The solid line is the approximation of Eq. (8); dashed lines are fits to power laws $\Gamma(\varepsilon = \hat{\varepsilon}) \sim \mu^{0.24 \pm 0.01}$ and $\Gamma(\varepsilon = 1) \sim \mu^{0.18 \pm 0.01}$. (b) Collapsing plots of $S(q)$ as a function of the rescaled variable $x = (q^2 - q_0^2)/(q_0 \Gamma)$ at $\varepsilon = \hat{\varepsilon}$ for $\mu = 10^{-2}$ (dotted line), $\mu = 10^{-3}$ (dashed line), and $\mu = 10^{-4}$ (long dashed line); the solid line is a squared Lorentzian curve $1/(1 + x^2)^2$.

the convection cell was increased linearly in time. This setup is similar to the annealing protocol in our simulations suggesting that the scaling found in those experiments can be explained within the Kibble-Zurek scenario as well.

Since the order parameter remains small up to $\varepsilon = \hat{\varepsilon}$, the observed scaling can be obtained from a simple linear approximation of Eq. (1). Fourier transforming the linearized SH-equation yields

$$\partial_t \hat{\phi}_{\mathbf{q}}(t) = [\mu t - (q_0^2 - \mathbf{q}^2)^2] \hat{\phi}_{\mathbf{q}}(t) + \hat{\eta}_{\mathbf{q}}(t), \qquad (2)$$

where $\hat{\phi}_{\mathbf{q}}(t)$ is the Fourier mode of the order parameter field with wave vector $\mathbf{q}$. Thus, the structure factor $S(q, t) \equiv \langle |\hat{\phi}_{\mathbf{q}}(t)|^2 \rangle$ is given by

$$S(q, t) = 2F e^{2\omega_q(t)} \int_{t_0}^{t} e^{-2\omega_q(s)} ds, \qquad (3)$$

where $\omega_q(t) \equiv \frac{1}{2}\mu(t^2 - t_0^2) - (q_0^2 - q^2)^2(t - t_0)$. The structure factor $S(q, t)$ is peaked around $q \simeq q_0$ [see Fig. 3(b)] and the time dependent width of this peak $\Gamma(t)$ is obtained from $S(q_0 \pm \frac{1}{2}\Gamma(t), t) \equiv \frac{1}{2}S(q_0, t)$. We find that $\Gamma(t)$ satisfies the implicit equation

$$\Gamma(t) = \left(\frac{\ln(2\alpha)}{2q_0^2 t} \right)^{1/2}, \qquad (4)$$

where $\alpha = 1 + O(\Gamma^2)$. Assuming that $S(q, t)$ is sharply peaked around q_0 (i.e., $\Gamma \ll 1$) and that it can be approximated by a squared Lorentzian around q_0 [8,9] [see Fig. 3(b)] we write

$$\langle \phi^2 \rangle = \sum_{\mathbf{q}} S(q, t) \simeq \frac{q_0 S(q_0, t)}{8(\sqrt{2} - 1)^{1/2}} \Gamma(t). \qquad (5)$$

Combining this result with the implicit equation $\langle \phi^2 \rangle = \delta \hat{\varepsilon}$, we find that $\hat{\varepsilon}$ satisfies

$$\hat{\varepsilon}^2 \simeq \mu \ln[(2F)^{-1} \delta q_0 C_0 \hat{\varepsilon}^{3/2}], \qquad (6)$$

where $C_0 \simeq 4.93$ is a numerical constant. Thus, the linear approximation leads, up to logarithmic corrections, to the scaling behavior $\hat{\varepsilon} \sim \mu^{1/2}$ predicted by the Kibble-Zurek scenario and confirmed by our simulations (see Fig. 1).

We now proceed to identify the typical length scale selected by the dynamics during the quench. A canonical measure for this length is the width of the structure factor [7–12]: in a defect-free domain the order parameter field takes the form

$$\phi(\mathbf{x},t) \simeq A(\mathbf{x},t)\cos[\mathbf{q}(\mathbf{x},t) \cdot \mathbf{x}] + \text{higher harmonics}, \quad (7)$$

where $A(\mathbf{x},t)$ and $\mathbf{q}(\mathbf{x},t)$ vary slowly within the domain. Thus, in the absence of any defects one expects the structure factor $S(q,t) = \langle |\hat{\phi}_{\mathbf{q}}(t)|^2 \rangle$ of an infinite system to be a delta function centered around $q = q_0$. When defects are present, the structure factor broadens around q_0 and the width Γ at half height can be used as a proxy for the length, i.e., we define $\xi \equiv \Gamma^{-1}$. Figure 3(a) shows the data for Γ at $\varepsilon = \hat{\varepsilon}$ and $\varepsilon = 1$ numerically obtained from a circular average of the structure factor. We find that $S(q,t)$ has a scaling form $S(q,t)/S(q_0,t) \simeq f((q^2 - q_0^2)/(q_0\Gamma))$ [see Fig. 3(b)] at least for a given (scaling) interval around $q = q_0 \simeq 1$. Results are thus independent of the threshold (half height) used to obtain Γ, provided the analysis is performed within this scaling region. At $\varepsilon = \hat{\varepsilon}$ we find $\xi \sim \mu^{-0.24 \pm 0.01}$ which again confirms the Kibble-Zurek prediction $\xi \sim \mu^{-1/4}$. Note that this scaling can be recovered within the linear approximation by combining Eqs. (4) and (6) to obtain

$$\Gamma(\hat{\varepsilon}) \simeq \mu^{1/4} \sqrt{\frac{\ln 2}{2q_0^2}} [\ln(\delta q_0 C_0 \hat{\varepsilon}^{3/2}(2F)^{-1})]^{-1/4}, \qquad (8)$$

which agrees with the Kibble-Zurek result up to logarithmic corrections and compares quantitatively well with the numerical data [see Fig. 3(a)].

We find, however, that right after the jump the absolute value of ξ decreases and then rapidly saturates to a value smaller than that at the jump. The data at any later instant (e.g., $\varepsilon = 1$) deviates from the Kibble-Zurek prediction in the regime of small μ, in fact in the interval $10^{-4} \leq \mu \leq 10^{-3}$ it can be fitted to $\xi \sim \Gamma^{-1} \sim \mu^{-0.18 \pm 0.01}$. To understand this apparent inconsistency, we first note that coarsening of the defect structure cannot be responsible for this effect, since $\xi(\varepsilon = \hat{\varepsilon}) > \xi(\varepsilon = 1)$. Instead, a possible explanation is given in Refs. [13,21]: the broadening of the spectrum, and hence the observed value of Γ is not only related to the spatial distribution of defects, but also to variations of the local wave number $q(\mathbf{x},t)$ within the defect-free domains. Using the numerical procedure suggested in Ref. [21] we find that although the distribution of local wave numbers $q(\mathbf{x},t)$ in Eq. (7) is centered around the expected value $q(\mathbf{x},t) = q_0$, it exhibits a finite width indicating variations in the actual val-

ues of $q(\mathbf{x},t)$. To quantify this effect we measure the RMS of those fluctuations, $\Delta q \equiv \langle [q(\mathbf{x},t) - q_0]^2 \rangle^{1/2}$, where the average extends over defect-free domains only. We find that Δq is a significant fraction of Γ for small values of μ, where Γ is small [see Fig. 3(a)]. Although, in principle, the observed value of Γ can be a complicated convolution of both the local variations of the value of $q(\mathbf{x},t)$ and the presence of defects, we have tried a simple linear ansatz to disentangle both contributions, i.e., $\Gamma = \Gamma_{\text{def}} + \Delta q$, where we assume that Γ_{def} is directly related to the spatial distribution of defects. In fact, the data for Γ_{def} at $\varepsilon = 1$ obtained using this simple ansatz can be fitted to a power law $\Gamma_{\text{def}} \sim \mu^{-0.24 \pm 0.01}$ and rescaled by a constant factor to collapse well with Γ taken at $\varepsilon = \hat{\varepsilon}$ as shown in Fig. 3(a). This indicates that the Kibble-Zurek scaling $\xi \sim \mu^{-1/4}$ might still hold at $\varepsilon = 1$, although it appears to be masked by local variations of the wave number [22].

An independent way of checking the Kibble-Zurek predictions is to measure the density of defects ρ created during the quench. Several methods have been devised to identify defects numerically [8–12]. Here we present results for two independent measures of the number of defects: the first one is based on the local amplitude of the order parameter field [9], while the second one relies on the local curvature of the observed stripes [11]. Far away from any defect the order parameter field $\phi(\mathbf{x},t)$ is of sinusoidal form (7), so that the local amplitude can be numerically estimated as $A^2(\mathbf{x},t) \simeq \phi(\mathbf{x},t)^2 + [\nabla \phi(\mathbf{x},t)]^2/q_0^2$. In equilibrium, it is found that $A^2(\mathbf{x},t) \simeq A_0^2 \equiv 4\varepsilon/3$ to lowest order in ε for a set of parallel stripes [2]. The density of defects ρ_a can thus be calculated using the filter $|[A^2(\mathbf{x},t) - A_0^2]/A_0^2| > \vartheta$, where ϑ is some threshold. The second method consists in numerically extracting the probability distribution $P(\kappa,t)$ of the local curvature $\kappa(\mathbf{x},t) = |\nabla \cdot \mathbf{n}(\mathbf{x},t)|$ of the stripe patterns [11]. Here $\mathbf{n} = \nabla \phi / |\nabla \phi|$ is the unit vector normal to the lines of constant ϕ. For a defect-free pattern, the curvature is zero, so again defect points can be identified as those with $\kappa(\mathbf{x},t) > \Theta$, where Θ is a given threshold. Thus the density of defects is $\rho_c = \int_\Theta^\infty P(\kappa,t) d\kappa$. In Fig. 2 we display typical configurations of the SH signal and the corresponding defect structures obtained using the first filter, demonstrating that this method can detect the defect structure efficiently. The thresholds ϑ and Θ are carefully chosen to be within the finite interval, in which our results for ρ_a and ρ_c are (up to a constant prefactor) independent of the particular choice of ϑ and Θ.

As shown in Fig. 4 the numerical values for ρ_c can be rescaled to agree very well with the density of defects obtained from the amplitude signal, ρ_a, so that (up to a constant factor) both methods independently yield the same density of defects. For relatively large values of μ, we find that the density scales like $\rho \sim \mu^{1/2}$ and also that $\rho \sim \Gamma_{\text{def}}^2$, as shown in Fig. 4. Consequently, if Γ_{def} is related to the density of defects, those should be pointlike for quick quenches. A simple inspection of the configurations after the jump confirms this picture, see Fig. 2. We observe that for small values of μ most of the defects are pointlike, while only a minor fraction is spatially extended. Only at small values of the
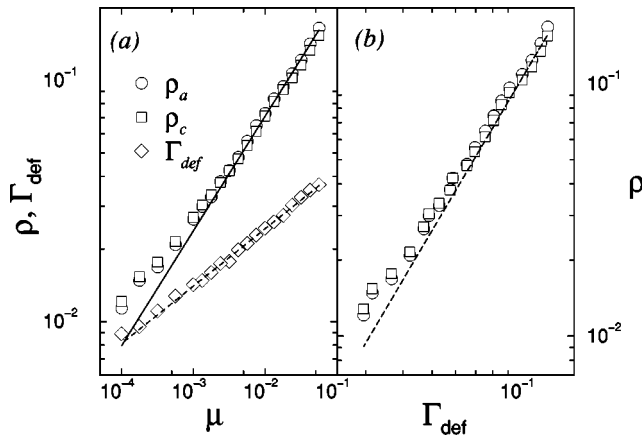
FIG. 4. (a) Density of defects ρ_a and ρ_c (rescaled to collapse with ρ_a) obtained at $\varepsilon=1$ (the data for $\mu>10^{-2}$ are taken at $\varepsilon=2$), and $\Gamma_{def}=\Gamma(\varepsilon=\hat\varepsilon)$ (in arbitrary units) as a function of μ. The solid line corresponds to $\rho\sim\mu^{0.48}$ and dashed line is $\Gamma_{def}\sim\mu^{0.24}$. (b) Density of defects as a function of Γ_{def}. The dashed line is $\rho\sim\Gamma_{def}^2$.

sweep rate does the density of defects deviate from the $\rho\sim\Gamma_{def}^2\sim\mu^{1/2}$ scaling, and we observe an increasingly significant amount of extended defects. If extended defects dominate over pointlike defects, a crossover to $\rho\sim\Gamma_{def}\sim\mu^{1/4}$ should be expected for small μ. Although a departure from the $\rho\sim\mu^{1/2}$ behavior is evident for slow quenches, our computational facilities at present do not allow us to give an accurate confirmation of this possible crossover.

In conclusion, we have confirmed the validity of the Kibble-Zurek picture for the creation of defects in the annealing of the SH equation. Specifically, we have identified a length scale $\xi\sim\Gamma_{def}^{-1}$ directly related to the density of defects, and found that it scales with the sweep rate as $\xi\sim\mu^{-1/4}$. For large values of μ, where most of the created defects are pointlike, we expect $\rho\sim\xi^{-2}$, a result which is observed in our simulations. However, for slow quenches, where an increasing fraction of extended defects is produced, we expect a deviation from this scaling law and a possible crossover to $\rho\sim\xi^{-1}$. We hope this work will stimulate other simulations of the SH model in order to confirm this picture.

Finally, we note that in studies of the coarsening in the SH model [6,11], it is observed that at large times defects are extended and that thus $\rho\sim\xi^{-1}$. Our study suggests that the presence of pointlike defects might be relevant, and thus some care has to be taken in the SH model when comparing the density of defects with the characteristic length observed in the system. We hope that taking into account this aspect together with the identification of the length scale associated with the density of defects as suggested in this paper might be useful to shed some light on the question of self-similarity in the coarsening process after an sudden quench of the SH system [23].

[1] P. M. Chaikin and T. C. Lubensky, *Principles of Condensed Matter Physics* (Cambridge University Press, Cambridge, 1995).

[2] M. Cross and P. Hohenberg, Rev. Mod. Phys. **65**, 851 (1993).

[3] E. Bodenschatz, W. Pesch, and G. Ahlers, Annu. Rev. Fluid Mech. **32**, 709 (2000).

[4] J. Swift and P.C. Hohenberg, Phys. Rev. A **15**, 319 (1977).

[5] M. Seul and D. Andelman, Science **267**, 476 (1995).

[6] A.J. Bray, Adv. Phys. **43**, 357 (1994).

[7] K. Elder, J. Viñals, and M. Grant, Phys. Rev. Lett. **68**, 3024 (1992); Phys. Rev. A **46**, 7618 (1992).

[8] M. Cross and D. Meiron, Phys. Rev. Lett. **75**, 2152 (1995).

[9] Q. Hou, S. Sasa, and N. Goldenfeld, Physica A **239**, 219 (1997).

[10] J. Christensen and A. Bray, Phys. Rev. E **58**, 5364 (1998).

[11] D. Boyer and J. Viñals, Phys. Rev. E **64**, 050101 (2001); **65**, 046119 (2002).

[12] H. Qian and G. F. Mazenko, Phys. Rev. E (to be published), e-print cond-mat/0210334.

[13] L. Purvis and M. Dennin, Phys. Rev. Lett. **86**, 5898 (2001).

[14] C. Harrison, D.H. Adamson, Z. Cheng, J.M. Sebastian, S. Set-huraman, D.A. Huse, R.A. Register and P. Chaikin, Science **290**, 1558 (2000).

[15] G. Ahlers, M.C. Cross, P.C. Hohenberg, and S. Safran, J. Fluid Mech. **110**, 297 (1981).

[16] T.W.B. Kibble, J. Phys. A **9**, 1387 (1976); Phys. Rep. **67**, 183 (1980); W.H. Zurek, Nature (London) **317**, 505 (1985); **368**, 292 (1994); Phys. Rep. **276**, 177 (1996).

[17] P. Laguna and W.H. Zurek, Phys. Rev. Lett. **78**, 2519 (1997); A. Yates and W.H. Zurek, *ibid.* **80**, 5477 (1998).

[18] G.D. Lythe, Phys. Rev. E **53**, R4271 (1996); E. Moro and G.D. Lythe, *ibid.* **59**, R1303 (1999).

[19] F. Liu and G.F. Mazenko, Phys. Rev. B **46**, 5963 (1992).

[20] S. Casado, W. González-Viñas, H. Mancini, and S. Boccaletti, Phys. Rev. E **63**, 057301 (2001).

[21] D. Egolf, I. Melnikov, and E. Bodenschatz, Phys. Rev. Lett. **80**, 3228 (1998).

[22] Note that directly at the jump striped patterns are not yet fully developed making the definition of local wave number, curvature and defects meaningless.

[23] T. Galla and E. Moro (unpublished).